# ChemComm

Accepted Manuscript


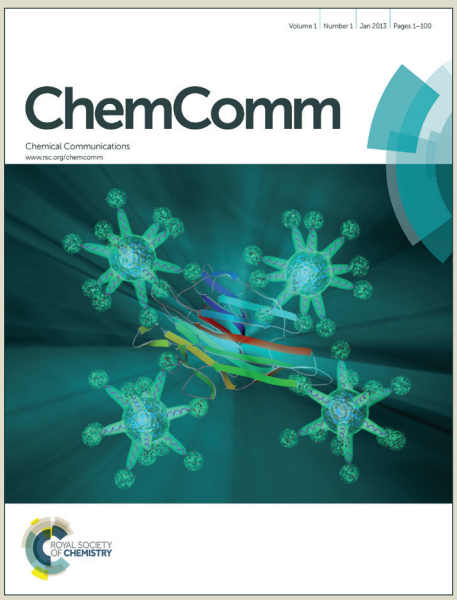





ROYAL SOCIETY OF CHEMISTRY

www.rsc.org/chemcomm

Journal Name

RSCPublishing

COMMUNICATION

# A New Enzyme-Free Quadratic SERS Signal Amplification Approach for Circulating MicroRNA Detection in Human Serum

Cite this: DOI: 10.1039/x0xx00000x

Received 00th January 2015,
Accepted 00th January 2015

DOI: 10.1039/x0xx00000x

www.rsc.org/

*Jing Zheng*[a,†], *Dandan Ma*[a,†], *Muling Shi*[a,†], *Junhui Bai*[b], *Yinhui Li*[a], *Jinfeng Yang*[c], *Ronghua Yang*[a,b,*]

**In this communication, we proposed a new enzyme-free quadratic SERS signal amplification approach for ultrasensitive detection of circulating miRNA in human serum. Combining with miRNA-triggered hybridization chain reaction and $Ag^+$-mediated cascade amplification, a limit of miRNA detection as low as 0.3 fM could be achieved. More importantly, our method is suitable for the direct detection of circulating miRNAs in human serum collected from patients of different stages of chronic lymphocytic leukemia(CLL).**

MicroRNAs (miRNAs) are short, endogenous, noncoding RNA of about 18-24 nucleotides (nt) that play important roles in normal and pathologic processes.[1-2] They can regulate gene activity through incorporation into an active RNA-induced silencing complex (RISC) and act to promote or repress cell proliferation, migration and apoptosis.[1-2] Recent studies have demonstrated that the distinct levels of miRNAs, particularly circulating miRNAs in serum, have a potential to become new biomarkers for cancer diagnosis and prognosis. Thus, sensitive and selective detection of multiplex miRNAs in biological fluids is of great significance in understanding biological functions of miRNAs and early diagnosis of cancers. Current widely used miRNA analysis methods, including Northern blotting and miRNA array technology,[3-4] could meet the detection requirement to some degree. However, due to the low abundance of miRNA in total RNA samples, these traditional methods have an intrinsic limitation in sensitivity, as one target molecule converts only one signal readout.

To achieve highly sensitive detection of miRNA, reverse transcription polymerase chain reaction (RT-PCR) have been employed and show high sensitivity (~100 fM) and specificity.[5] Nonetheless, this method is susceptible to the inhibition of the PCR process by the cell extract and the related electrophoresis procedures is laborious and time consuming. Alternatively, various PCR-free methods mainly based on enzyme-assisted amplification have been developed.[6-9] For instance, Ye *et al* took advantage of the duplex-specific nuclease (DSN) to create a single-step signal amplifying mechanism and demonstrate its application for rapid detection of miRNAs.[10] However, great progress in improving the sensitivity and specificity of these methods still hindered by the single-step signal amplification. To further improve the sensing sensitivity for miRNA, Xia *et al* proposed a quadratic amplification strategy based on polymerase-aided strand-displacement polymerization and exonuclease-assisted template recycling which could achieve rapid and highly sensitive detection of miRNAs.[11] All of these strategies indeed provided useful platforms for the detection of miRNA and related research, however, the possibility of practical application is hampered due to the high cost and complicated manipulation of protein enzyme. Thus, an alternative enzyme-free strategy to multi-step amplify the signal for miRNA detection is still urgently needed.

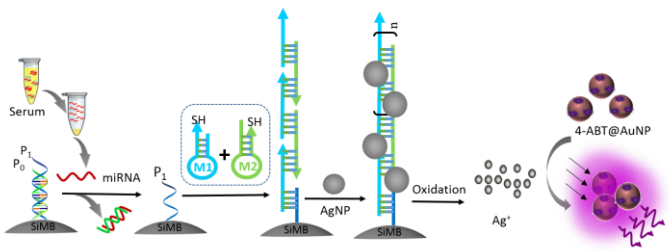


**Scheme 1**. Design scheme of enzyme-free quadratic SERS signal amplification for circulating microRNA detection in human serum *via* miRNA-triggered hybridization chain reaction and $Ag^+$-mediated cascade amplification.

In this communication, we proposed an enzyme-free quadratic signal amplification strategy *via* target miRNA-triggered hybridization chain reaction and ions-mediated cascade amplification. Hybridization chain reaction (HCR) is an enzyme-free, room temperature linear amplification approach which is simple in operation and cost-effective only using the DNA single strand for *in situ* adjustment of the length of double strand DNA (dsDNA).[12-13] When these formed long dsDNA are used in bioanalysis, the signaling molecules can be attached with precisely controlled density, thus would be beneficial for the final amplification efficiency.[14] In our design, as shown in Scheme 1, we fabricated the target circulating miRNA-induced long self-assembled DNA polymer *via* HCR on the surface of silica microbeads (SiMBs) to induce multiple AgNPs conjugation, which worked as a primary amplification element. Since one AgNP can be dissolved into numerous $Ag^+$ which can control the gaps between neighboring 4-aminobenzenethiol (4-ABT) encoded gold nanoparticles (AuNP@4-

ABT) to form "hot-spot" and produce enhanced surface-enhanced Raman spectroscopy (SERS) signal,[15] quadratic amplification endows achieving a limit of miRNA detection as low as 0.3 fM. More importantly, our method can be further used for the direct detection of circulating miRNAs in serum collected from patients of different stages of diffuse large B cell lymphoma (CCL).

As a first step towards this goal, HCR, one of the most attractive enzyme-free DNA assemble strategy was chose to fabricate long DNA polymer. In HCR, a initiator and two species of sulfydryl-labeled DNA hairpin probes, M1 and M2, that can coexist stably in solution are rationally designed (the initiator sequence was named $P_1$, all sequences were shown in Table S1, ESI). HCR between $P_1$, M1 and M2 was first examined by ethidium bromide (EB)-stained agarose gel electrophoresis in solution (Fig. S1). In the absence of $P_1$, HCR between M1 and M2 was inhibited, and only a bright band of M1 or M2 could be observed, as shown in lane 2. However, emission bands of high-molecular weight structures could also be observed in lanes 3-6, indicating the successful growth of long polymer in the presence of initiator. Under these circumstances, a low concentration of $P_1$ was able to trigger a proportionately small chain reaction of alternating kinetic escapes by M1 and M2, resulting in the formation of a long DNA polymer. Then, AgNPs were prepared and characterized according to the reported method to fabricate AgNPs-conjugated long DNA polymer *via* Ag-S bond. Transmission electron microscopy (TEM) demonstrates a size distribution of AgNPs from 10 to 15 nm, most being 12 nm (Fig. S2A). The UV-vis absorption spectrum shows a maximal absorption central at 396 nm (Fig. S2B), which can be attributed to the surface plasmon resonance of AgNPs. To fabricate AgNPs-loaded long DNA polymer, the AgNPs were conjugated to the DNA polymer using Au-S bond. After incubation and centrifugation at 5000 rpm for 10 min, a process which has been optimized to attain the best separation effect, representative TEM image clearly demonstrated that the AgNPs were self-assembled along with the hetero-chains of the DNA polymer (Fig. S3). These collective results confirmed that $P_1$ had actually assisted in the self-assembly of nicked-DNA polymer structure and, subsequently, the AgNPs conjugates.

In order to attain preferable separating effect and eliminate the false positive signal generated from the complex biological background, SiMB was employed to serve as an effective substrate. Since miR-21 is a potential cancer biomarker which has been identified with elevated expression levels in serum correlated with numerous tumour, including breast, liver, ovarian, pancreatic, and brain, in comparison to their normal counterparts,[16] we chose it as the model target in our design. The biotin-labeled initiator probe $P_1$ designed having a complementary sequence to capture probe ($P_0$, sequences were shown in Table S1) was immobilized on the surface of streptavidin coated-SiMBs through streptavidin-biotin interaction. Upon addition of $P_0$, it can hybridize with initiator probe $P_1$ to form duplex strand. In the presence of target miR-21, the $P_0$ are partially displaced from the surface of SiMBs, which causes the $P_1$ to be liberated as single strand. In this case, the $P_1$ in solution can pair with the sticky end of M1, which undergoes an unbiased strand-displacement interaction to open the hairpin. The newly exposed sticky end of M1 nucleates at the sticky end of M2 and opens the hairpin to expose a sticky end on M2. This sticky end is identical in sequence to the initiators strands. In this way, each initiator strand $P_1$ propagates a HCR event between alternating M1 and M2 to form a nicked double-helix. The sulfhydryl group on one building block is thus brought into close proximity to other such moieties. Thus, numerous sulfhydryl functional groups are self-assembled together, providing potential binding sites for AgNPs *via* specific Ag-S bond. After incubated with AgNPs and centrifugated at 1000 rpm for 10 min, representative scanning electron microscope (SEM) images showed that the conjugated AgNPs were very closely aggregated on the surface of SiMBs, and a few bright spots appeared in the image (Fig.1A). However, the control experiment, in which miR-21 was absent, showed no aggregates on the surface of SiMB (Fig.1A, Inset). The elemental composition determined by energy-dispersive X-ray spectroscopy (EDX) further evidenced the coexistence of C, O and Ag elements (Fig.1B) on the surface of SiMB. We next used atomic force microscope (AFM) images to characterize the surface features of the conjugated AgNPs aggregates, which exhibited a mean height between 100-120 nm (Fig. 1C, D).

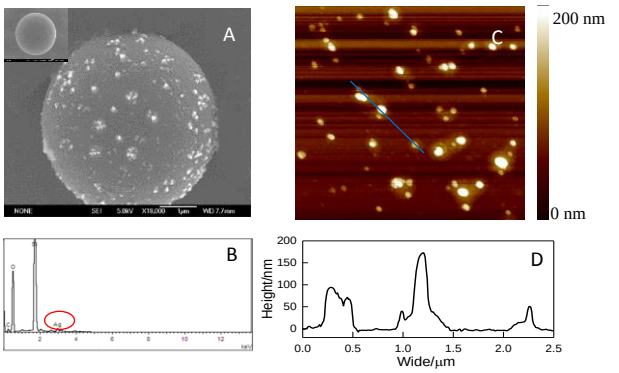


**Fig. 1** (A) Representative SEM image of the long DNA polymer-conjugated AgNPs on the surface of SiMBs in the presence of miR-21 after HCR. Inset: SEM image of the surface of SiMB in the absence of miR-21. (B) EDX of the formed long DNA polymer-conjugated AgNPs under the STEM pattern and red circle represents Ag element. (C) AFM topographic images of (A), and (D) is the corresponding height profiles of the the formed long DNA polymer-conjugated AgNPs on the surface of SiMBs. Scale area: 1.0×1.0 μm.

As the important signal transduction element, large size of AuNPs were synthesized by two-step seed mediated method.[17] As characterized by TEM, AuNPs were shown to be uniform and mono-dispersed with an average size of 60 ± 4 nm and the UV-vis absorption spectrum shows that λmax= 550 nm was mainly attributed to surface plasmon resonance of AuNPs (Fig. S4). Then, the AuNPs were incubated with 4-ABT to form AuNPs@4-ABT through Au-S bond of mercapto group of 4-ABT and AuNPs surface. To avoid the unexpected aggregation caused by the high concentration of 4-ABT, the AuNPs were not fully covered with 4-ABT. In our experiment, 4-ABT and diluted AuNPs were incubated with a molar ratio of 280:1 and the surface coverage of 4-ABT molecules on AuNPs was evaluated to be 2.85 pmol/cm$^2$(details was shown in ESI) , assuming perfect adsorption probability and an occupation area of 20 Å$^2$ for 4-ABT according to our previous report.[15]

Since we have discovered that the introduction of $Ag^+$ to AuNPs@4-ABT solution could cause AuNPs aggregation by forming N→Ag←N coordination compounds, and obvious SERS spectrum induced by the subsequent formed "hot-spot" could be observed. Firstly, aggregation of AuNPs@4-ABT mediated by $Ag^+$ was evidenced by the TEM image and UV-vis spectra in Fig. S5. Then, Fig. S6 demonstrated that when the $Ag^+$ concentration increased to about $1.0\times10^{-7}$ M, or even higher, the SERS signal remained fairly constant and a plateau

was reached due to the interaction between $Ag^+$ and AuNPs@4-ABT finally reaching the equilibrium state in terms of kinetics and thermodynamics. Based on this, the long DNA polymer-conjugated AgNPs were dissolved by hydrogen peroxide ($H_2O_2$) to attain numerous $Ag^+$ in our design. As shown in Fig. S7, the vast majority of bright spots disappeared and the surface of SiMB were similar with bare ones. Therefore, these DNA self-assemble-mediated AgNPs-encoded SiMBs have the potential of providing numerous $Ag^+$ for substantial signal amplification.

Then, we measured the SERS spectra of our constructed HCR-assisted ions-mediated cascade amplification nanoplatform before and upon miR-21 addition under the optimized condition according to the previous report.[15] As shown in Fig. 2, no obvious SERS signals could be observed by the weak surface plasmon field in the absence of miR-21(curve a). However, upon addition of miR-21 to the mixture, a stronger SERS signal was demonstrated (curve b). To further demonstrate the SERS signal amplification by HCR, a control experiment was designed by directly employing M1. A short DNA hybrid was formed among initiator, M1 upon addition of miR-21, and only few AgNPs were loaded, resulting in relatively weak SERS signal state after AgNPs dissolution (curve c). In this case, the value of $I/I_0$ dropped to 5.78 upon the addition of 100 pM miR-21, demonstrating the effective signal enhancement of our proposed platform, where $I_0$ and $I$ were the SERS intensities at 1440 $cm^{-1}$ in the absence and presence of miR-21, respectively. Besides, two additional types of AgNP, 4 nm and 30 nm (UV-spectra were shown in Fig. S8) were investigated to attain ideal SERS signal enhancement of our constructed HCR-based ions-mediated cascade amplification. As shown in Fig. S9, considering the conjugation efficiency of AgNPs and the number of $Ag^+$ release, 12 nm AgNPs was chose in the subsequent experiment.

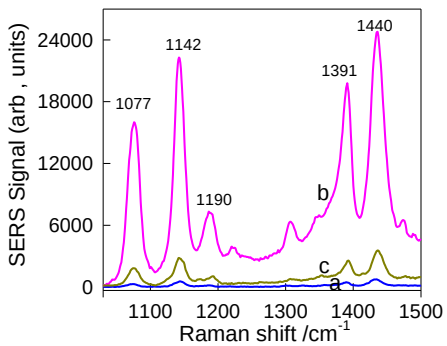


**Fig. 2** SERS spectra obtained from HCR-assisted ions-mediated cascade SERS amplification approach in the absence (curve a) and presence of 50 pM miR-21 (curve b and curve c). Curve c was obtained by employing M1 only without HCR. The concentrations of SiMB-$P_0$/$P_1$, M1, and M2 were 500 nM, 1.0 μM and 1.0 μM, respectively. The amount of AgNPs and 4-ABT/AuNPs were excess. All error bars were obtained through the detection of six parallel samples.

We next measured the SERS signal improvement as functions of miR-21 concentration. Fig. 3A illustrated the SERS intensity increased dramatically with the increasing concentration of miR-21. Change of Raman intensity at 1440 $cm^{-1}$ with and without miR-21 termed as $I/I_0$ was quantitatively analyzed and showed a good linear fit to the concentration of miR-21 in the range from 1 fM to 10 pM, as shown in Fig.3B. The limit of detection, based on 3 times the signal-to-noise level, was estimated to be ~0.3 fM, which is comparable with the other reported system (Table S2), demonstrating its satisfactory sensitivity to apply in real sample.

A significant challenge for miRNA analysis is the ability to distinguish many highly similar sequences that differ by only a few nucleotides. Therefore, we performed a series of contrast experiments using single mismatched miR-21(SM-21) and miR-141 (sequences were shown in Table S1) to evaluate the specificity of this proposed miRNA assay method. As shown in Fig. S10, there was very weak SERS intensity enhancement ($I/I_0$) in the presence of interfering miRNA compared with the complementary target miR-21. Besides, nearly negligible SERS change was observed upon the addition of the mixture containing SM-21 and miR-141 compared with the blank. This provides an excellent selectivity in the fabrication of miR-21 SERS detector based on long DNA polymer-conjugated AgNPs and $Ag^+$-mediated cascade amplification.

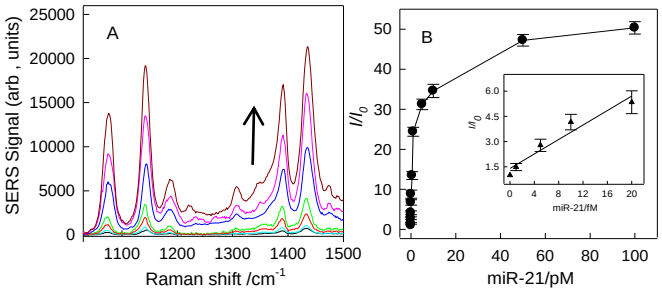


**Fig. 3** Performances of SERS detection of miR-21 in buffer solution. (A) SERS spectra of HCR-aided ions-mediated cascade amplification SERS detector upon addition of different concentrations of miR-21. The arrow indicates the signal changes as increases in the miR-21 concentration (0, 0.001, 0.005, 0.01, 0.5, 1.0 and 10 pM). (B) Dependence of SERS intensity enhancement of the 1440 $cm^{-1}$-band, $I/I_0$, on different concentrations of miR-21 in buffer solution. Inset: $I/I_0$ plotted against the concentration ranging from 0 to 20 fM. The measuring conditions as shown in Fig. 2. All error bars were obtained through the detection of six parallel samples.

Recent research demonstrated that the expression levels of miR-21 in serum might provide a new diagnostic approach for chronic lymphocytic leukemia (CCL).[18] In this design, we investigated the feasibility of our proposed method for the direct detection of miRNAs in serum. Circulating miRNAs are associated with protein complexes and exosomes,[19] which are conducive to their high stability. We first released miRNAs from the enclosure of protein and exosome using heat treatment and then detected miR-21 in the supernatant of serum lysate. In Fig. S11, the peak current measured from serum sample of a CCL patient is substantially higher than that from a healthy donor (curve a). Such a difference suggests that the expression level of miR-21 has been up-regulated in the CCL patient. To further demonstrate the clinical relevance of our method, we carried out assays of miRNA-21 in serum samples from multiple healthy donors and CCL patients. Due to the ideal separation effect of SiMBs, the concentrations of miR-21 in serum were further calculated according to the calibration curve in Fig. 3B. As shown in Fig. 4, the results obtained by HCR-assisted ions-mediated cascade amplification are in good agreement with those obtained by quantitative real-time PCR (qPCR, experimental details was shown in ESI), further confirming the accuracy of the HCR-based ions-mediated cascade amplification SERS assay. Meanwhile, it was observed that the circulating miR-21 have exhibited an increased expression of varying degrees, in the chronic lymphocytic leukemia Rai stage 3 (CLL-3) serum compared to chronic lymphocytic leukemia Rai stage 1(CLL-1) and healthy serum, which is coincided with the previous report and demonstrating the applicability of this

approach in clinical diagnosis.[18] These results demonstrate that the proposed method can directly quantify miRNA in serum with great reliability, thus holding a great potential for further applications in the clinic diagnosis of leukaemia.

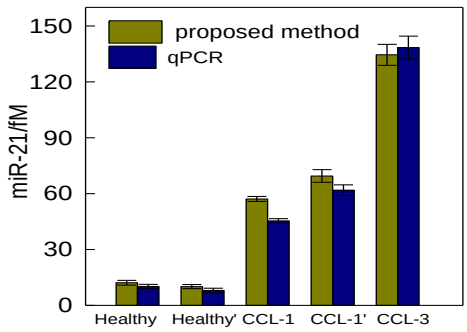


**Fig. 4** Detection of CCL-related miR-21 in human serum samples. Bars represent the concentrations of miR-21 in serum from two healthy donors (normal and normal') and three CCL patients donors (CCL-1, CCL-1' and CCL-3) detected with qPCR (blue bars) and our proposed HCR-based ions-mediated cascade amplification SERS detection (grass green bars), respectively. Error bar show the standard deviation of six experiments.

## Conclusions

In conclusion, we have developed an enzyme-free quadratic amplified miRNA SERS sensing assay *via* target miRNA-triggered HCR and $Ag^+$-mediated cascade amplification, and further applied it for sensitive and selective measurement of CCL-related miRNAs (miR-21) in serum. The result demonstrated that the detection limit is as low as 0.3 fM, and it also could be used for the direct detection of circulating miRNAs in serum collected from patients of different stages of chronic lymphocytic leukemia (CLL). The good performance of this approach was ascribed to (1) two steps for signal amplification and (2) the entire process is enzyme-free, inexpensive and simple to prepare. We believe that this strategy would add a new concept to design PCR-free, enzyme-free, an effective tool for simultaneous high sensitive quantitative analysis of multiple biomarkers in serum and supplies valuable information for biomedical research and clinical early diagnosis of cancer.

This work was supported by the financial support through the National Natural Science Foundation of China (21405038, 21135001, 21305036) and the Fundamental Research Funds for the Central Universities.

## Notes and references

[a]*State Key Laboratory of Chemo/Biosensing and Chemometrics, College of Chemistry and Chemical Engineering, Hunan University. Changsha, 410082, China;* [b]*School of Chemistry and Biological Engineering, Changsha University of Science and Technology, Changsha, 410004, China;* [c]*Department of Anesthesiology, The Affiliated Cancer Hospital of Xiangya School of Medicine, Central South University, Changsha, 410013, China;*
*E-mail: Yangrh@pku.ed.cn*
*†J. Z, D. D. M and M. L. S contributed equally to the work.*
*Electronic Supplementary Information (ESI) available: More experimental details and spectroscopic data as noted in text.*

[1] R. C. Lee, R. L. Feinbaum and V. Ambos, *Cell*, 1993, **75**, 843.
[2] J. Lu, G. Getz, B. L. Ebert, R. H. Mak, A. A. Ferrando, J. R. Downing and T. R. Golub, *Nature*, 2005, **435**, 834.
[3] M. Lagos-Quintana, R. Rauhut, W. Lendeckel and T. Tuschl, *Science*, 2001, **294**, 853.
[4] J. M. Thomson, J. Parker, C. M. Perou and S. M. Hammond, *Nat. Methods.*, 2004, **1**, 47.
[5] C. Chen, D. A. Ridzon, A. J. Broomer and K. J. Guegler, *Nucleic Acids Res.* 2005, **33**, e179.
[6] Y. Cheng, X. Zhang, Z. Li, X. Jiao, Y. Wang and Y. Zhang, *Angew. Chem.,Int. Ed.*, 2009, **48**, 3268.
[7] H. Jia, Z. Li, C. Liu and Y. Cheng, *Angew. Chem., Int. Ed.*, 2010, **49**, 5498.
[8] J. VanNess, L. K. VanNess and D. J. Galas, *Proc. Natl. Acad. Sci. U. S. A.*, 2003, **100**, 4504.
[9] C. Y. Hong, X. Chen, J. Li, J. H. Chen, G. N. Chen and H. H. Yang, *Chem. Commun.*, 2014, **50**, 3292.
[10] B. C. Yin, Y. Q. Liu and B. C. Ye, *J. Am. Chem. Soc.* 2012, **134**, 5064.
[11] R. X. Duan, X. L. Zuo, S. T. Wang, L. Jiang, C. H. Fan and F. Xia, *J. Am. Chem. Soc.*, 2013, **135**, 4604.
[12] R. M. Dirks and N. A. Pierce, *Proc. Natl. Acad. Sci. U. S. A.*, 2004, **101**, 15275.
[13] J. Xu, J. Wu, C. Zong, H. X Ju and F. Yan, *Anal. Chem.*, 2013, **85**, 3374.
[14] J. Zheng, Y. P. Hu, J. H. Bai, R. H. Yang and W. H. Tan, *Anal. Chem.*, 2014, **86**, 2205.
[15] M. L. Shi, J. Zheng, Y. J. Tan, G. X. Tan, J. S. Li, Y. H. Li and R. H. Yang, *Anal. Chem.*, 2015, **87**, 2734.
[16] K. Zen and C.Y. Zhang, *Med. Res. Rev.*, 2012, **32**, 326.
[17] M. A. Cortez, C. Bueso-Ramos, J. Ferdin, A. K. Sood and G. A. Calin, *Nat. Rev. Clin. Oncol.*, 2011, **8**, 467.
[18] C. H. Lawrie, S. Gal, H. M. Dunlop, B. Pushkaran, A. P. Liggins, K. Pulford, A. H. Banham and F. Pezzella, *Br J Haematol*, 2008, **141**, 672.
[19] K. R. Brown, D. G. Walter and M. J. Natan, *Chem. Mater.*, 1999, **12**, 306.